Twenty-year operation of the Cryospheric Environment Simulator

Osamu ABE[1]* and Kenji KOSUGI[1]
1 Shinjo Cryospheric Environment Laboratory, Snow and Ice Research Center, National Research Institute for Earth Science and Disaster Resilience, 1400 Tokamachi, Shinjo 996-0091, Japan
* abeosamu1950@gmail.com

(Received October 12, 2016; Revised manuscript accepted March 1, 2019)

Abstract

The operational results for the Cryospheric Environment Simulator (CES) of the National Research Institute for Earth Science and Disaster Resilience (NIED) compiled over a 20-year period from October 1997 to March 2017, during which a total of 598 projects were conducted, are reported herein. These projects were instigated by four types of institutions: official institutes, universities, companies, and the NIED itself. In terms of international cooperative use, 12 institutes or universities from 9 countries have conducted various investigations using the CES. The present specifications, performances, and operations of CES are described herein; some of the scientific results and future considerations are also presented.

Key words: simulator, cold room, wind tunnel, artificial snow

1. Introduction

The Cryospheric Environment Simulator (CES) was established in 1997 at the Shinjo Cryospheric Environment Laboratory, Snow and Ice Research Center, National Research Institute for Earth Science and Disaster Resilience (NIED). The CES is a large state-of-the-art facility available for domestic and international cooperative use that can reproduce a variety of cryospheric environmental conditions, including snowfall, that are similar to those occurring in natural environments.

Using this simulator, researchers or engineers can conduct diverse research projects related to basic and applied disaster mitigation as well as cryospheric environmental studies. Higashiura *et al.* (1997) reported on the planning and development of the CES; however, there had been no English language report of its measured specifications or post-construction operations.

2. Specifications

The CES controls air temperature and humidity in a 167.5 m^2 cold room in which liquid or solid precipitation and solar radiation can be controlled over a 3 × 5 m^2 experimental table. There are six cooling units in the cold room; five work to maintain the air temperature and the sixth to defrost. Thus, the air temperature can be continuously controlled over a long duration. The air conditioning system was designed such that the heating and cooling rates of the air temperature are ±10 °C h^{-1}. While Higashiura *et al.* (1997) reported on the specifications used in the initial planning of the CES, there have been a number of upgrades and revisions over the years. The present specifications are shown in Table 1. For example, the maximum available humidity was changed from 100 to 70 % because humidity at extremely low temperatures is very difficult to control.

Table 1

2.1 Snowfall simulators

Two snowfall simulators are provided: type A produces dendritic snowflakes and type B produces ice particles (Fig. 1). In type A, dendritic ice crystals are produced on a special mesh that is vertically stretched by two rotating rollers (Fig. 2; Umezawa and Seki, 1997). The aggregation of dendritic ice crystals is similar to that of a measured dendritic snowflake. In type B, fine ice particles are produced using a two-phase nozzle and flow along air streams onto the same mesh as that of type A. Then, cohesive ice particles are tapped by a bar behind the mesh (Fig. 3; Seki, 1996). Examples of both types of snow particles are shown in the upper right of Fig. 1. Initial densities immediately following the snowfall are 20 kg m^{-3} for type A and 200 kg m^{-3} for type B. The maximum snowfall intensities as precipitation are 1 mm h^{-1} for type A and 5 mm h^{-1} for type B, as shown in Table 1. The continuous operating time of both simulators is 72 h (3 days) depending on the water supply system.

Fig. 1

Fig. 2

Fig. 3

2.2 Rainfall and solar simulators

Rainfall and solar radiation are individually controlled over the experimental table. The rainfall simulator nozzles were upgraded after a heavy rainfall observed during February 2014 on the Kanto Plain (Fig. 4). Rainfall intensity is controlled at 13 mm h^{-1} with five steps. To monitor the precipitation, a rain gauge (10 cm in diameter) and a balance with a vessel (20 × 20 cm^2) are provided (Fig. 5). The rain gauge counts droplets of water gathered by a funnel such that the recording time of a pulse produced by a droplet may include a delay. One pulse of the rain gauge refers to 0.011 mm of precipitation. There is no delay in the recording time for the balance with a vessel. There are water draining channels on the floor in the cold room. The solar simulator changes the solar radiation from 50 to 1000 W m^{-2} at a step of 50 W m^{-2} (Fig. 6). The solar simulator can be inclined up to 45° from the experimental table.

Fig. 4

Fig. 5

Fig. 6

2.3 Wind tunnel

The wind tunnel is a vertical return flow type. Wind speed is controlled via a wind tunnel that has a 1 × 1 m^2 cross-section and a test section length of 14 m (Figs. 1 and 7). The maximum wind speed is 20 m s^{-1} in the center of the wind tunnel. To reproduce blowing snow, two different small snowfall machines, situated on top of the wind tunnel, can be used individually to accumulate snow via different processes (Fig. 8). The first snowfall machine is a vibrational type that agitates a wire mesh to sieve snow particles, and the second is a brush rotational type that rotates four brushes within the open space of a horizontal cylinder to sieve snow particles (Abe *et al.*, 2009). Furthermore, to reproduce drifting snow, two types of snow seeders, a rotating-brush type or a reciprocating type, can be installed at the windward base of the wind tunnel to control the seeding rate of the snow particles (Fig. 9). The first can produce a thick drifting snow layer and the second a denser drifting

Fig. 7

Fig. 8

Fig. 9

snow than the first.

2.4 Equipment

Normally, the experimental table is set at a horizontal position to form a snowpack or to set up instruments; however, it can be inclined up to 45°. A 3-m-wide blower drives wind over the experimental table. The wind speed is controlled from 0 to 10 m s^{-1} at the discharge opening.

Many types of equipment are also available to CES users, including a polarized microscope, a thermal imager, and a high-speed video camera (Max. 2000 frames s^{-1}). Figure 10 shows the control room. All parameters previously described are controlled by an operator sitting at the control desk. A technician supports researchers or engineers in many types of tasks, for example, planning experiments and preparation and data collection.

Fig. 10

3. Performance

The performance of the CES is a function of the accuracy of the values for each simulator and the responses of its individual components. Furthermore, simultaneous functioning of the simulators may interfere with their optimal performance. In planning an experiment, users need to know how rapidly a parameter changes, and the extent of influence of each parameter on the others. Table 2 summarizes the times for preparation and stabilization for each parameter after it is set. Snowfall and rainfall simulators that use considerable water at controlled temperatures take a long time to initiate precipitation. Accordingly, time series data measured for four typical cases are shown in the following sections; namely, snowfall (type A and type B), rainfall, and solar radiation. In these cases, the air temperature was always simultaneously controlled.

Table 2

3.1 Snowfall (type A) and air temperature

The preparation time needed to initiate the type A snowfall (dendritic crystals) is approximately 4 h. Figure 11 shows time series data for precipitation, air temperature, and humidity as the first two parameters are controlled. As can be seen, the snowfall simulator preparation began at 09:40 and the strongest snowfall (level 5) commenced 3.5 h later at 13:15. Level 5 snowfall intensity represents the maximum precipitation of 1 mm h^{-1}, and levels 1 to 5 are divided into 5 steps for maximum precipitation. Precipitation measured using a balance with a vessel approaches a constant value 1 h later because it is necessary to slowly roll the special mesh to produce the dendritic crystals in the simulator (Fig. 2). For the same reason, when users change the snowfall intensity to a different level, the simulator requires 1 h to approach the constant intensity. However, when the snowfall rate is reduced, the time required to produce a constant snowfall is shorter. Notably, after the snowfall simulator is stopped, precipitation continues for approximately 15 min to clear the dendritic crystals formed on the mesh.

Fig. 11

The air temperature gradually decreases from +12 to -10 °C over 2 h during snowfall preparation. After the measured air temperature reaches the desired value of -10 °C, the fluctuation in the air temperature is ±0.5 °C. Notably, the type A snowfall simulator has a limitation of a maximum temperature of -10 °C. The humidity is not controlled; the measured level fluctuates at approximately 60 % during snowfall.

3.2 Snowfall (type B) and air temperature

The type B snowfall simulator uses two-phase water nozzles and high-pressure air to create ice particles (Fig. 3). Figure 12 shows the time series precipitation, air temperature, and humidity data. The snowfall intensity (level) can rapidly change depending on the water supply system. At first, the snowfall intensity is set to level 3 at 13:15, then changes to level 1 at 14:00, then to level 5 with a maximum intensity at 14:30, and finally stops at 15:30. The level 5 maximum snowfall intensity represents a precipitation of 5 mm h^{-1}, and levels 1 to 5 are divided into 5 steps for maximum precipitation. Similar to that of the type A snowfall simulator, this simulator also needs a preparation time of approximately 4 h. In this case, the air temperature is maintained at a constant of -2 °C, which is the maximum temperature possible in the simulator, and the fluctuation is maintained within $\pm$0.5 °C of the desired value.

Fig. 12

3.3 Rainfall and air temperature

Rainfall intensity can be set at 6 different levels: 1 to 5 and continuous mode C. Levels 1 to 5 correspond to the precipitation of 0.4, 0.8, 1.2, 1.6, and 2 mm h^{-1}. The rainfall simulator consists of 28 nozzles, each of which has a constant water supply rate. The droplet sizes of the simulator range from 60 to 410 μm (Kobayashi *et al.*, 2002). When in use, the simulator controls the interval times for each level; however, a continuous mode is provided to reproduce a heavier rainfall. Its precipitation intensity is 5 mm h^{-1}. Figure 13 shows controlled rainfall and air temperature records for the period from 09:15 to 12:15 on February 24, 2016. In this case, precipitation levels varied among levels 1, 3, 5, and C. At first, the rainfall started at level 1 with the lowest intensity at 09:15, changed to level 3 at 10:15, to level 5 at 11:00, then to the continuous mode (C in Fig. 13) at 11:45, and finally stopped at 12:15. The rain gauge did not detect the beginning of the weak rainfall, because the small funnel of the rain gauge cannot collect sufficient water droplets for measurements.

Fig. 13

However, after the aforementioned measurements were conducted, all of the nozzles were replaced during March 2016 because heavier rainfall was needed to create conditions for a “rain on snow” experiment. The new setup is capable of creating a maximum precipitation intensity of 13 mm h^{-1} in the continuous mode, approximately three times greater than that of the former version. The droplet sizes of the upgraded simulator range from 70 to 320 μm approximately.

3.4 Solar radiation and air temperature

The solar simulator is usually simultaneously controlled with air temperature. Figure 14 shows time series data for the desired and measured values for solar radiation and air temperature simultaneously controlled from 14:15 to 16:30 on February 26, 2016. After the desired solar radiation value is changed, there is a large initial gap between it and the measured value, but the measured value eventually becomes constant. The solar simulator can be set to the desired value in steps of 50 W m^{-2}.

Fig. 14

4. Operations

4.1 Proposals

Each year, call for research proposals is issued on our website (http://www.bosai.go.jp/seppyo/) at the beginning of January. The CES is open for use to selected parties and can also be used for cooperative research efforts. After all proposals have been received, negotiations are conducted to schedule each approved project. Finally, each proposal is evaluated by the CES steering committee, which consists of professional glaciologists, engineers, governmental officials, and members of the NIED. Some projects have continued for as long as two or three years; however, most projects can be conducted within a week's time during each fiscal year.

4.2 Support

An operator and a technician are available to support each experiment. Electrical supply, at 200 V, is available in two phases (Max. 50 A) and three phases (Max. 50 A), while 100 V is available in two phases (Max. 50 A). All electrical outlets are Japanese standard, but there are two terminals that can be used to directly connect to the 200-V power supply. To support visiting collaborators, we also provide a three-bedroom guesthouse with a kitchen and a bathroom.

4.3 Maintenance

Because the CES consists of numerous systems and parts, many of which need to be serviced or regularly replaced, maintenance stand-downs are scheduled twice per year to ensure that the simulator operates without problems during the remaining time. The first is a full three-week maintenance period during March and the second is a two-week maintenance period during September. However, despite our comprehensive maintenance efforts, unexpected troubles have sometimes occurred.

4.4 Costs

Costs are estimated by considering three factors: the amount of electric power and water expended during the experiment, facility depreciation (including maintenance), and salary expenses for the technician and the operator. Cooperative use can reduce the cost by one-half, and expenses for universities or national institutes for cooperative use may be waived.

5. Results

5.1 General results

A total of 598 projects, including cooperative and commercial research efforts, and the NIED's own original studies were conducted using the CES during October 1997 to March 2017. Most projects were associated with snow and ice disaster prevention, but others focused on earth science (Fig. 15a). Most research themes could be classified into one of six categories (Fig. 15b); however, the number of projects associated with snow and ice accretion has increased, primarily because of the recent heavy snowfalls that have occurred in normally snow-free areas as well as traditionally snowy areas (Kamiishi and Nakamura, 2016).

Fig. 15

The projects were approximately balanced among four user types, including the NIED's own research efforts, as shown in Fig. 15c. Of these, 79 projects conducted by institutes and 222 by

Fig. 16

universities were cooperative domestic research efforts, while 148 projects were conducted by domestic companies to develop new sensors or instruments relating to snow and ice, including commercial non-cooperative projects. Additionally, the CES hosted international cooperative projects involving 12 institutes or universities from 9 countries.

Figure 16 shows the yearly variations in the number of projects conducted at the CES. As shown, the average number of projects per year has been approximately 30. As previously mentioned, five weeks of routine maintenance are scheduled each year, and from three to five days of downtime are required each year to recover from unexpected troubles.

5.2 Scientific results

A wealth of papers based on the results of CES projects have been published in numerous journals according to the biennial report of the CES (Shinjo Cryospheric Environment Laboratory, 2015). This includes 266 papers in Japanese and 39 papers in English. In addition, graduate students have presented 36 theses in Japanese and 1 thesis in English, based on CES results, thereby proving that the facility provides strong support for university education programs. The following is a short overview of some of these papers based on this research field:

(1) Physical properties of snow

Sokratov and Sato (2000, 2001) investigated the interaction between wind and snow on the snow surface using the wind tunnel. Abe (2001) conducted creep experiments and numerical simulations of very light artificial snow packs, while Nakamura *et al.* (2001) and Tanikawa *et al.* (2006) investigated the spectral albedo of the snow surface using different snow types. Uemura *et al.* (2005) evaluated isotopic fractionation of water during snow crystal growth using the snowfall simulator, in which snow crystals are formed by vapor and supercooled droplets of water onto a special mesh (Fig. 2).

(2) Drifting snow

Font *et al.* (2001) compared the collection efficiency of three net-type collectors to that of a snow particle counter. Meanwhile, Sato *et al.* (2001, 2004a) and Kosugi *et al.* (2004) confirmed the basic parameters of drifting snow such as saltation length. Sato *et al.* (2008) investigated the mechanisms of fracturing and accumulation of snowflakes on snow surfaces. In more recent research, Okaze *et al.* (2012) assessed drifting snow development in a boundary layer, while Nishimura and Ishimaru (2012) developed an automatic blowing-snow station based on laboratory experiments. Nishimura *et al.* (2014) and Nemoto *et al.* (2014) improved the momentum exchange between snow particles and airflow.

In addition, Tominaga *et al.* (2012, 2013) conducted particle image velocimetry (PIV) measurements to understand snow saltation phenomena in the wind tunnel. Okaze *et al.* (2009) and Tominaga *et al.* (2009, 2011) presented numerical models, including computational fluid dynamics (CFD) models, and compared their calculated results to the measured results obtained using the wind tunnel.

(3) Avalanches

Hirashima *et al.* (2009) proposed a new parameter to improve the shear strength of depth hoar based on laboratory experiments. For earthquake-induced snow avalanches, a dynamic method for measuring the shear strength of snow was proposed by Nakamura *et al.* (2010), while Podolskiy *et al.* (2010) conducted an experimental study on the same topic. Meanwhile, Ito *et al.* (2012) investigated changes in snow strength using both snowfall and rainfall simulators.

(4) Snow and ice accretion

Kimura *et al.* (2009) and Mughal *et al.* (2016) evaluated icing sensors in the wind tunnel, while Kimura *et al.* (2013) verified the effect of snow accumulation on ultrasonic wind sensors. From an earth science perspective, Suzuki *et al.* (2008) evaluated snow accumulation on evergreen needle-leaf trees using the snowfall simulator. The number of cooperative and commercial use projects increased following the heavy snowfall that occurred around the central part of Honshu Island in 2014, particularly for communication systems as traffic signals.

(5) Snow accumulation

Sakurai *et al.* (2012) presented a practical method for predicting rooftop snow accumulation based on wind pressure characteristics.

(6) Others

Sato *et al.* (2004b) and Nakai *et al.* (2012) constructed and improved a snow disaster forecasting system based on field observations and laboratory experiments.

6. Future considerations

Through the wide variety of projects conducted during the 20 years that the CES has been in operation, we determined that the following modifications to its procedures, specifications, and operations will be necessary for the future:

6.1 Procedures

(1) Standardization

In the evaluation of sensors or equipment, different results may occur according to the test procedures used. Therefore, standardization of a common test procedure would be needed for each evaluation. The CES is capable of standardization because test conditions can be accurately controlled.

(2) Approach to microstructure

Physical properties of snow are strongly related to microstructure; for example, quantitative representation of irregularly shaped snow particles, specific surface area, and effective particle radius.

Advanced instruments such as X-ray computed microtomography or magnetic resonance imaging installed and implemented with the CES will contribute to this research field.

6.2 Specifications

(1) Parameter expansion

For severe conditions observed in nature, from its initiation to the present, the CES has expanded its capability; for example, the maximum precipitation intensity has expanded from 5 mm h^{-1} to 13 mm h^{-1}. However, the maximum wind speed remains at 20 m s^{-1}; it should be increased to at least 30 m s^{-1}.

(2) Wet snowfall reproduction

Recent extra-tropical cyclones have resulted in wet snowfalls in normally snow-free areas as well as in traditionally snowy areas, even during Japan's mild winter seasons, thereby resulting in a number of disasters related to snow accretion. Accordingly, to clarify the mechanisms involved, a wet snowfall simulator is needed.

(3) Different types of snow crystals

In 2014, it was observed that numerous loose snow avalanches occurred because of an extremely fragile layer forming just after a huge snowfall over the central part of the main Japanese island of Honshu. In this case, 'non-dendritic crystals', such as column, bullet, plate, and crossed plate shapes, formed at relatively low temperatures in high clouds were observed in the neighboring district (Ishizaka *et al.*, 2015). To investigate the mechanisms involved, it will be necessary to design and install a new snowfall simulator that can produce these types of snow crystals.

6.3 Operations

(1) Work crew

Currently, two staff members, a technician and an operator, are on duty during each project and they wish to accomplish a series of experiments for the project without any failure. However, with an eye towards reducing their mental and physical stress while also improving operational flexibility, a work crew of at least three staff members is preferable.

(2) Project merging

The CES has recently received so many proposals each year that it will be necessary to conduct negotiations in a manner that encourages two or three similar projects to be simultaneously performed.

7. Conclusion

Snow sciences have significantly progressed following the establishment of the CES; the results of various projects conducted using our simulator have been used to accurately predict snow and ice disasters (Sato *et al.,* 2004b; Nakai *et al.,* 2012). CES advantages include the ability to produce snowfall and fresh snow regardless of season, repeatability with high accuracy, and ample technical support. It is our target to improve all these aspects of CES performance in the near future.

Acknowledgments

The authors are grateful to the anonymous reviewer and the editor, Dr. Yamaguchi S., for their constructive comments that significantly contributed to improving the manuscript. We would also like to thank the following staff members of the CES over the last 20 years; Sato A., Sato T., Ishizaka M., and Kamiishi I. for their management; Nemoto M., Sato K., Adachi S., Nakamura K., and Kamata Y. for their cooperation; Yamaguchi S., Nakai S., Motoyoshi H., Hirashima H., Yamashita K., and Ito Y. for their counterpart of cooperative uses; Mochizuki S. and Togashi K. for their technical support; Takeda T. and Okawa G. for their helpful operation; and Yuki H., Nakagawa A. and Matsuda Y. for their administrative assistance. The CES was constructed under the supervision of the Tohoku District Bureau of the Ministry of Land, Infrastructure, Transport and Tourism (MLIT). This report is dedicated to the memory of the late Dr. Higashiura M., who was the founding director and guiding spirit behind the construction of the CES.

References

Abe, O. (2001): Creep experiments and numerical simulations of very light artificial snowpacks. *Ann. Glaciol.*, **32**, 39-43, doi: 10.3189/172756401781819201.

Abe, O., Mochizuki, S., Kosugi, K., Nemoto, M. and Sato, T. (2009): Snowfall seeders and drifting snow seeder of the wind tunnel, CES (in Japanese). *Summaries of JSSI & JSSE Joint Conference on Snow and Ice Research-2009/Sapporo*, p.92, doi: 10.14851/jcsir.2009.0.78.0.

Font, D., Sato, T., Kosugi, K., Sato, A. and Vilaplana, M. (2001): Mass-flux measurements in a cold wind tunnel: comparison of the mechanical traps with a snow-particle counter. *Ann. Glaciol.*, **32**, 121-124, doi: 10.3189/172756401781819102.

Higashiura, M., Abe, O., Sato, T., Numano, N., Sato, A., Yuuki, H. and Kosugi, K. (1997): Preparation of an experimental building for snow and ice disaster prevention. *Snow Engineering-Recent Advances*, ed. by M. Izumi, T. Nakamura and R. L. Sack, Rotterdam, 605-608.

Hirashima, H., Abe, O., Sato, A. and Lehning, M. (2009): An adjustment for kinetic growth metamorphism to improve shear strength parameterization in the SNOWPACK model. *Cold Reg. Sci. Technol.*, **59**, 169-177, doi: 10.1016/j.coldregions.2009.05.001.

Ishizaka, M., Fujino, T., Motoyoshi, H., Nakai, S., Nakamura, K., Shiina, T. and Muramoto, K. (2015): Characteristics of snowfalls and snow crystals caused by two extratropical cyclones passing along the Pacific Ocean side of Japan on February 8 and 14-15 observed in Niigata district, 2014 -in relation to frequent occurrence of avalanches in Kanto-Koshin areas- (in Japanese with English abstract). *J. Jpn. Soc. Snow and Ice (Seppyo)*, **77**, 285-302.

Ito, Y., Matsushita, H., Hirashima, H., Ito, Y. and Noro, T. (2012): Change in snow strength caused by rain. *Ann. Glaciol.*, **53**, 1-5, doi: 10.3189/2012AoG61A027.

Kamiishi, I. and Nakamura, K. (2016): Snow disaster caused by a cyclonic heavy snowfall in February, 2014, and countermeasures taken by the NIED and its future direction for disaster prevention (in Japanese with English abstract). *Natural Disaster Research Report*, **49**, 1-10.

Kimura, S., Sato, T., Yamagishi, Y. and Morikawa, H. (2009): Evaluation of ice detecting sensors by icing wind tunnel test. *Proceedings of the 13th International Workshop on Atmospheric Icing of Structures*, http://www.iwais2009.ch/index.php%3Fid=44.html.

Kimura, S., Yamagishi, Y., Morikawa, H., Kojima, T., Sato, T., Aalto, T., Valo, H. and Hietanen, J. (2013): De-icing testing and development of ultrasonic wind sensor for cold climate. *Winter Wind 2013 International Wind Energy Conference*, http://www.winterwind.se/sundsvall-2014/presentations-2013/.

Kobayashi, S., Satow, A., Abe, O., Miyakoshi, H., Ishimaru, T. and Maruyama T. (2002): A measurement method of liquid water content of fog using a precipitation gauge (in Japanese). *Annual Report of Research Institute for Hazards in Snowy Areas, Niigata University*, **24**, 103-106, http://hdl.handle.net/10191/39251.

Kosugi, K., Sato, T. and Sato, A. (2004): Dependence of drifting snow saltation lengths on snow surface hardness. *Cold Reg. Sci. Technol.*, **39**, 133-139, doi: 10.1016/j.coldregions.2004.03.003.

Mughal, U.N., Virk, M.S., Kosugi, K. and Mochizuki, S. (2016): Experimental validation of icing rate using rotational load. *Cold Reg. Sci. Technol.*, **127**, 18-24, doi: 10.1016/j.coldregions.2016.03.012.

Nakai, S., Sato, T., Sato, A., Hirashima, H., Nemoto, M., Motoyoshi, H., Iwamoto, K., Misumi, R., Kamiishi, I., Kobayashi, T., Kosugi, K., Yamaguchi, S., Abe, O. and Ishizaka, M. (2012): A Snow Disaster Forecasting System (SDFS) constructed from field observations and laboratory experiments. *Cold Reg. Sci. Technol.*, **70**, 53-61, doi: 10.1016/j.coldregions.2011.09.002.

Nakamura, T., Abe, O., Hasegawa, T., Tamura, R. and Ohta, T. (2001): Spectral reflectance of snow with a known grain-size distribution in successive metamorphism. *Cold Reg. Sci. Technol.*, **32**, 13-26, doi: 10.1016/S0165-232X(01)00019-2.

Nakamura, T., Abe, O., Hashimoto, R. and Ohta, T. (2010): A dynamic method to measure the shear strength of snow. *J. Glaciol.*, **56**, 333-338, doi: 10.3189/002214310791968502.

Nemoto, M., Sato, T., Kosugi, K. and Mochizuki, S. (2014): Effects of snowfall on drifting snow and wind structure near a surface. *Boundary-Layer Meteorology*, **152**, 395-410, doi: 10.1007/s10546-014-9924-4.

Nishimura, K. and Ishimaru, T. (2012): Development of an automatic blowing-snow station. *Cold Reg. Sci. Technol.*, **82**, 30-35, doi: 10.1016/j.coldregions.2012.05.005.

Nishimura, K., Yokoyama, C., Ito, Y., Nemoto, M., Naaim-Bouvet, F., Bellot, H. and Fujita, K. (2014): Snow particle speeds in drifting snow. *J. Geophys. Res.: Atmos.*, **119**, 9901-9913, doi: 10.1002/2014JD021686.

Okaze, T., Tominaga, Y., Mochida, A., Ito, Y., Nemoto, M., Yoshino, H. and Sato, T. (2009): Numerical modelling of drifting snow around buildings. *Proceedings 6th International Symposium on Turbulence, Heat and Mass Transfer*, CD-ROM.

Okaze, T., Mochida, A., Tominaga, Y., Nemoto, M., Sato, T., Sasaki, Y. and Ichinohe, K. (2012): Wind tunnel investigation of drifting snow development in a boundary layer. *J. Wind Engi. Indus. Aerody.*, **104-106**, 532-539, doi: 10.1016/j.jweia.2012.04.002.

Podolskiy, E.A., Nishimura, K., Abe, O. and Chernous, P.A. (2010): Earthquake-induced snow avalanches: II, Experimental study. *J. Glaciol.*, **56**, 447-458, doi: 10.3189/002214310792447833.

Sakurai, S., Abe, O. and Joh, O. (2012): Practical method for predicting snow accumulations on roofs based on wind pressure characteristics. *Proceedings of 7th International Conference on Snow Engineering*, **7**, 463-475.

Sato, T., Kosugi, K. and Sato, A. (2001): Saltation layer structure of drifting snow observed in wind tunnel. *Ann. Glaciol.*, **32**, 203-208, doi: 10.3189/172756401781819184.

Sato, T., Kosugi, K. and Sato, A. (2004a): Development of saltation layer of drifting snow. *Ann. Glaciol.*, **38**, 35-38, doi: 10.3189/172756404781815211.

Sato, A., Ishizaka, M., Shimizu, M., Kobayashi, T., Nishimura, K., Nakai, S., Sato, T., Abe, O., Kosugi, K., Yamaguchi, S. and Iwamoto, K. (2004b): Construction of snow disaster forecasting system in Japan. *Snow Engineering*, **5**, 235-238.

Sato, T., Kosugi, K., Mochizuki, S. and Nemoto, M. (2008): Wind speed dependences of fracture and accumulation of snowflakes on snow surface. *Cold Reg. Sci. Technol.*, **51**, 229-239, doi: 10.1016/j.coldregions.2007.05.004.

Seki, M. (1996): Artificial snowfall and snow making machines (in Japanese), *Refrigeration (Reito)*, **71**, 65-72.

Shinjo Cryospheric Environment Laboratory (2015): Report of experiments in the Cryospheric Environment Simulator (in Japanese). *Snow and Ice Research Center, National Research Institute for Earth Science and Disaster Resilience*, *Shinjo,* 69pp.

Sokratov, S.A. and Sato, A. (2000): Wind propagation to snow observed in laboratory. *Ann. Glaciol.*, **31**, 427-433, doi: 10.3189/172756400781820020.

Sokratov, S.A. and Sato, A. (2001): The effect of wind on the snow cover. *Ann. Glaciol.*, **32**, 116-120, doi: 10.3189/172756401781819436.

Suzuki, K., Kodama, Y., Yamazaki, T., Kosugi, K. and Nakai, Y. (2008): Snow accumulation on evergreen needle-leaved and deciduous broad-leaved trees. *Boreal Environment Research*, **13**, 403-416.

Tanikawa, T., Aoki, T., Hori, M., Hachikubo, A., Abe, O. and Aniya, M. (2006): Monte Carlo simulations of spectral albedo for artificial snowpacks composed of spherical and non-spherical particles. *Applied Optics*, **45,** 5310-5319, doi: 10.1364/AO.45.005310.

Tominaga, Y., Okaze, T., Mochida, A., Nemoto, M. and Ito, Y. (2009): Prediction of snowdrift around a cube using cfd model incorporating effect of snow particles on turbulent flow. *APCWE-Ⅶ*, CD-ROM.

Tominaga, Y., Okaze, T. and Mochida, A. (2011): CFD modelling of snowdrift around a building: An overview of models and evaluation of a new approach. *Building and Environment,* **46**, 899-910, doi: 10.1016/j.buildenv.2010.10.020.

Tominaga, Y., Okaze, T., Mochida, A., Nemoto, M., Sato, T. and Sasaki, Y. (2012): PIV measurements of snow particle velocity in a boundary layer developed in a wind tunnel. *Proceedings of 7th International Conference on Snow Engineering*, **7**, 273-279.

Tominaga, Y., Okaze, T., Mochida, A., Sasaki, Y., Nemoto, M. and Sato, T. (2013): PIV measurements of saltating snow particle velocity in a boundary layer developed in a wind tunnel. *J. Visual.*, **16**, 95-98, doi: 10.1007/s12650-012-0156-8.

Uemura, R., Matsui, Y., Yoshida, N., Abe, O. and Mochizuki, S. (2005): Isotopic fractionation of water during snow formation: Experimental evidence of kinetic effect. *Polar Meteorol. Glaciol.*, **19**, 1-14.

Umezawa, K. and Seki M. (1997): Large quantities snow making of singular crystal (rotation ventilation filter method) (in Japanese). *Proceedings of 1997 Cold Regions Technology Conference*, **13,** 12-16.

Table and figure captions

Table 1. Present CES specifications.

Table 2. Times for preparation and stabilization.

Fig. 1. Two types of snowfall simulators installed on the third floor (original illustration by M. Miura). Type A is fixed, and type B is temporarily at a position just under type A, the latter is used as required. The two circles in the upper right show optical micrographs of the snowfall particles.

Fig. 2. Schematic of type A snowfall simulator with 3 units. There are 12 units in the simulator installed on the third floor.

Fig. 3. Schematic of type B snowfall simulator with 2 units. There are 10 units in the simulator installed onto a carrier on the third floor.

Fig. 4. Rainfall simulator installed on a carrier at the top of the first floor. Twenty-eight nozzles are laid out in 4 rows and 7 columns on the carrier. The large circle refers to the enlarged image of a nozzle shown in the small circle.

Fig. 5. Rain gauge (left) and balance with a square vessel (right).

Fig. 6. Solar simulator. Solar radiation is controlled by the number of lamps that illuminate the object.

Fig. 7. Wind tunnel with a scale model of the object in the drifting snow layer. The test sections of both sides are comprised of transparent windows and all of the 2-m-wide front windows can be opened.

Fig. 8. Small snowfall machines used to sieve snow particles into the wind tunnel from the top window. Left: vibrational type, Right: rotating-brush type. Bottom figures show the snowfall machine schematics.

Fig. 9. Snow seeders in the wind tunnel. Left: rotating-brush type, Right: reciprocating type. Bottom figures show the snow seeder schematics. Dimensions of the sample box for both types are 0.2 m in length × 0.77 m in width × 0.3 m in depth.

Fig. 10. CES Control room. An operator (left) monitors the control panel and a technician (left back) supports data collection for the collaborators who typically provide their original instruments (right). The cold room can be seen through the window on the left.

Fig. 11. Time series data for desired and measured precipitation of snowfall A and air temperature, in addition to measured humidity.

Fig. 12. Time series data for desired and measured precipitation of snowfall B and air temperature, in addition to measured humidity.

Fig. 13. Time series data for precipitation and air temperature. The numbers indicate the rainfall simulator level used to control the precipitation.

Fig. 14. Time series data for desired and measured solar radiation and air temperature controlled simultaneously.

Fig. 15. Overview of the research field, theme, and institution.

Fig. 16. Institutional categorization of projects conducted at the CES.

Table 1. Present CES specifications.

Element	Value	Description
Max. temperature (℃)	25	Highest value happens usually in melting season.
Min. temperature (℃)	-30	Sintering speed of snow particles becomes enough slowly.
Max. humidity (%)	70	Technical limit of vapor supply system.
Min. humidity (%)	20	Lowest value happens usually in inland areas.
Max. wind speed ($m\ s^{-1}$)	20	Highest value happens usually during drifting snow.
Max. solar radiation ($W\ m^{-2}$)	1000	Highest value at latitude 60° north in summer.
Max. snow precipitation of type A ($mm\ h^{-1}$)	1	Normal value happens in snowy regions.
Max. snow precipitation of type B ($mm\ h^{-1}$)	5	Large value sometimes happens in snowy regions.
Max. rain precipitation ($mm\ h^{-1}$)	13	Upgraded after the heavy rainfall during February 2014 on the Kanto Plain.

Half width

Table 2. Times for preparation and stabilization.

Parameter	Preparation (h)	Stabilization (h)
Air temperature	-	*a
Humidity	-	0.2～0.5
Snowfall (type A)	～4	< 1
Snowfall (type B)	～4	0.25
Rainfall	1～2	< 0.1
Solar Radiation	-	0.25～0.3
Wind speed	-	0.015

*a: Changing rate is ±10 ℃ h^{-1}.

Half width

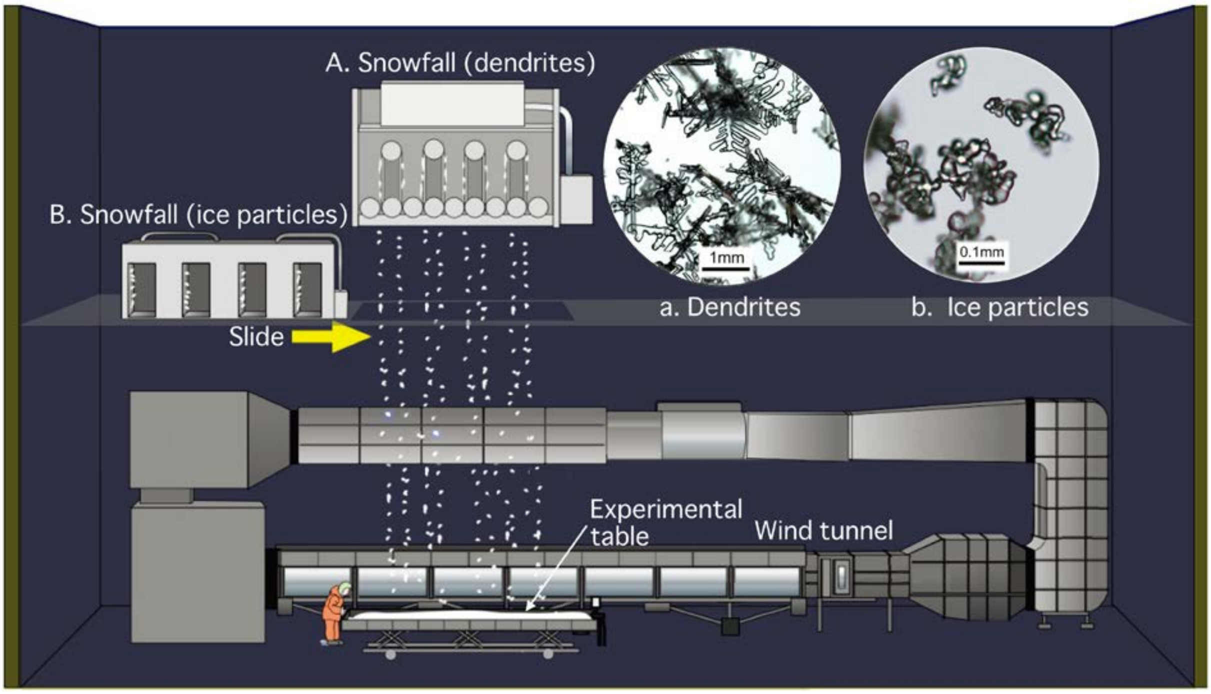

Fig. 1. Two types of snowfall simulators installed on the third floor (original illustration by M. Miura). Type A is fixed, and type B is temporarily at a position just under type A, the latter is used as required. The two circles in the upper right show optical micrographs of the snowfall particles.

Full width

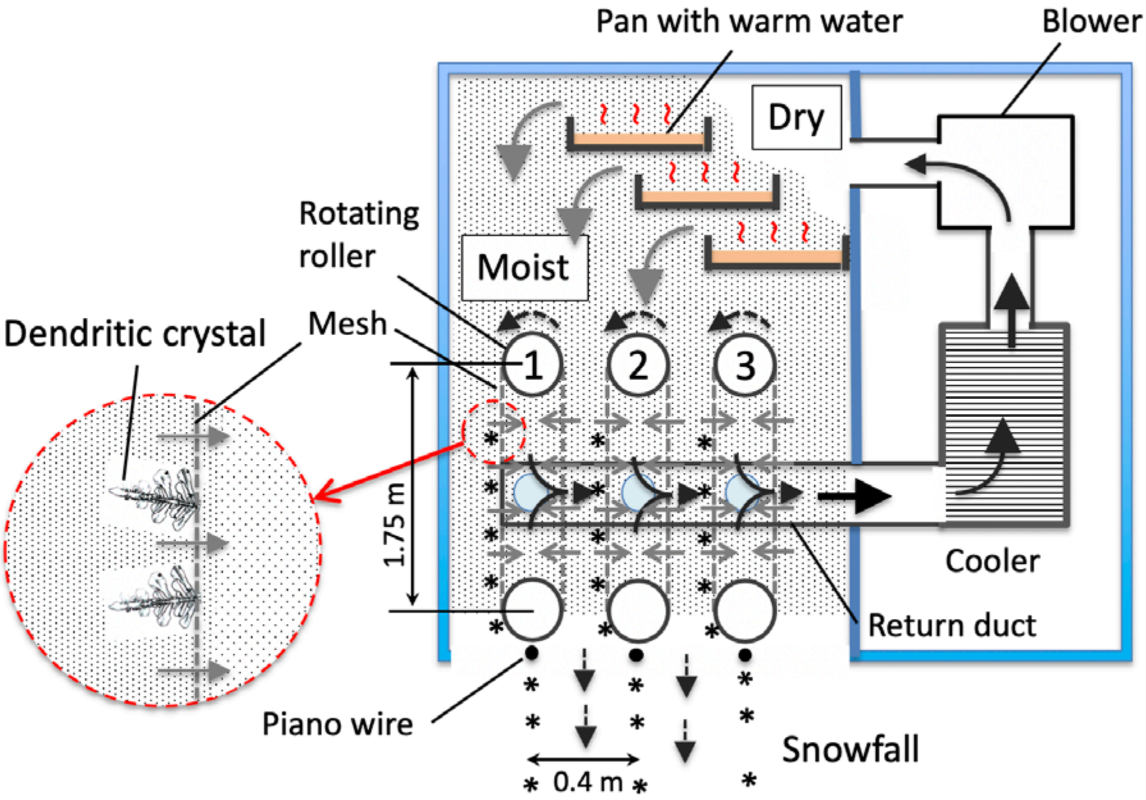

Fig. 2. Schematic of type A snowfall simulator with 3 units. There are 12 units in the simulator installed on the third floor.

Full width

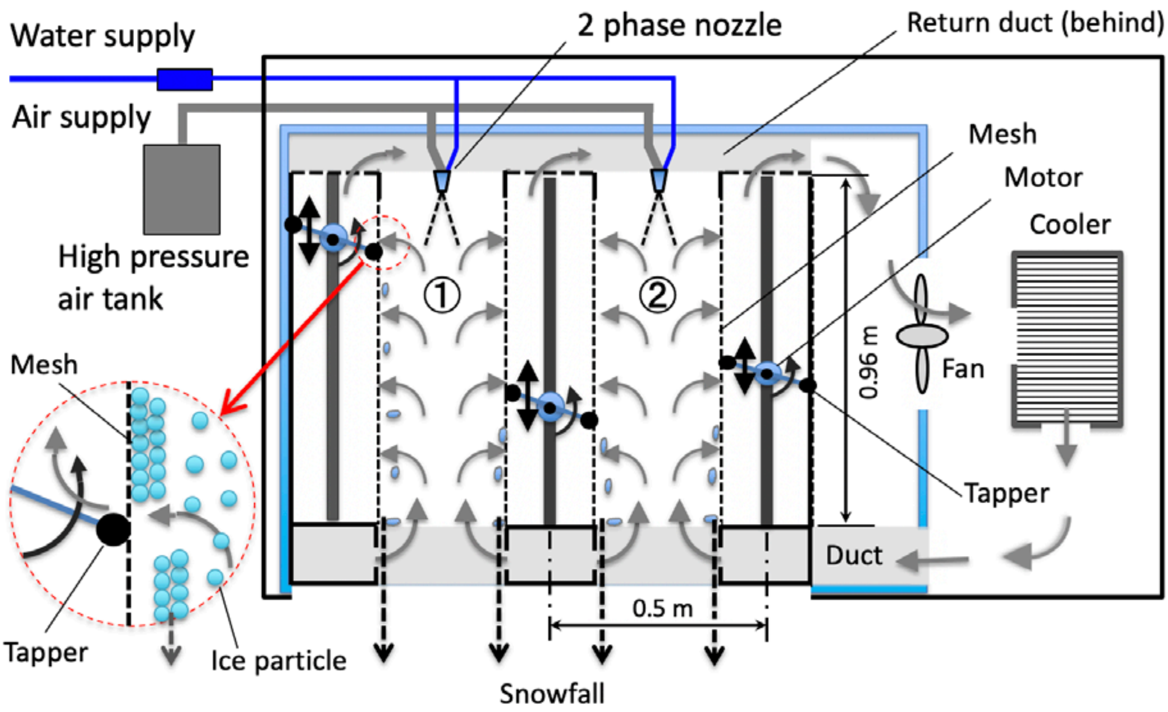

Fig. 3. Schematic of type B snowfall simulator with 2 units. There are 10 units in the simulator installed onto a carrier on the third floor.

Full width

Fig. 4. Rainfall simulator installed on a carrier at the top of the first floor. Twenty-eight nozzles are laid out in 4 rows and 7 columns on the carrier. The large circle refers to the enlarged image of a nozzle shown in the small circle.

Half width

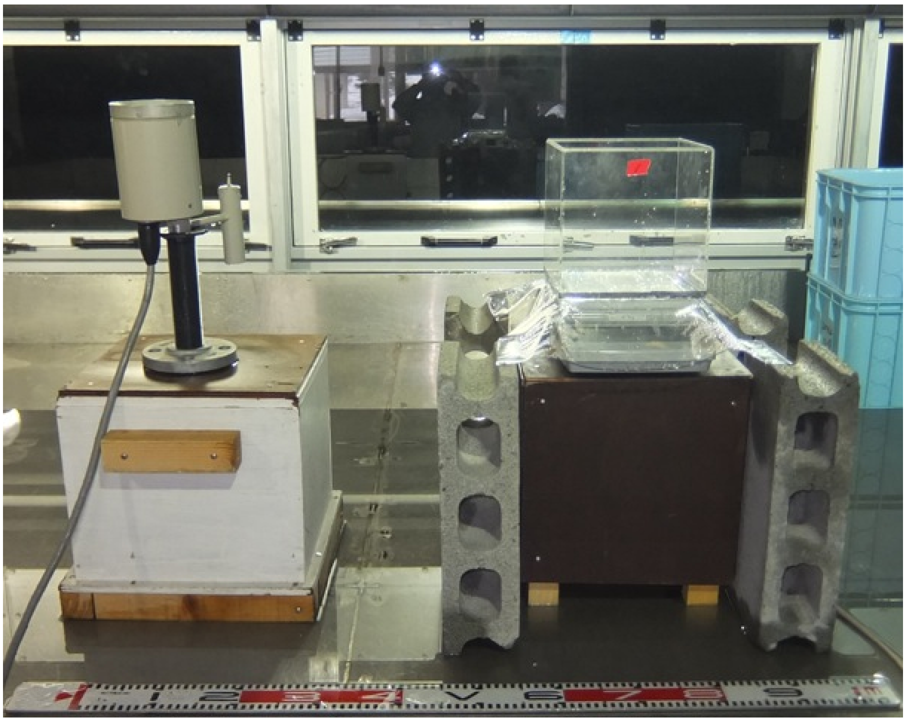

Fig. 5. Rain gauge (left) and balance with a square vessel (right).

Half width

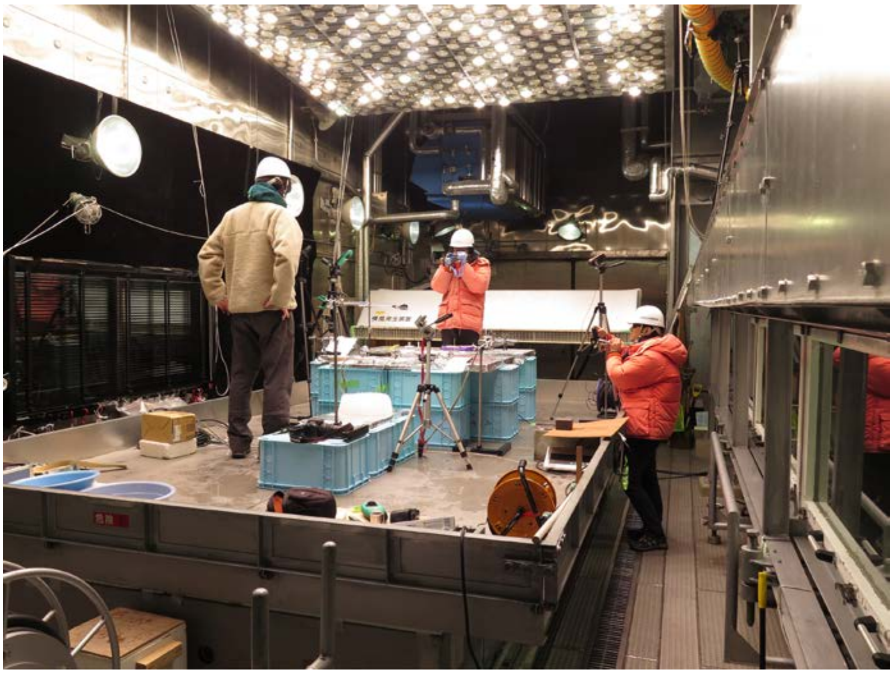

Fig. 6. Solar simulator. Solar radiation is controlled by the number of lamps that illuminate the object.

Half width

Fig. 7. Wind tunnel with a scale model of the object in the drifting snow layer. The test sections of both sides are comprised of transparent windows and all of the 2-m-wide front windows can be opened.

Half width

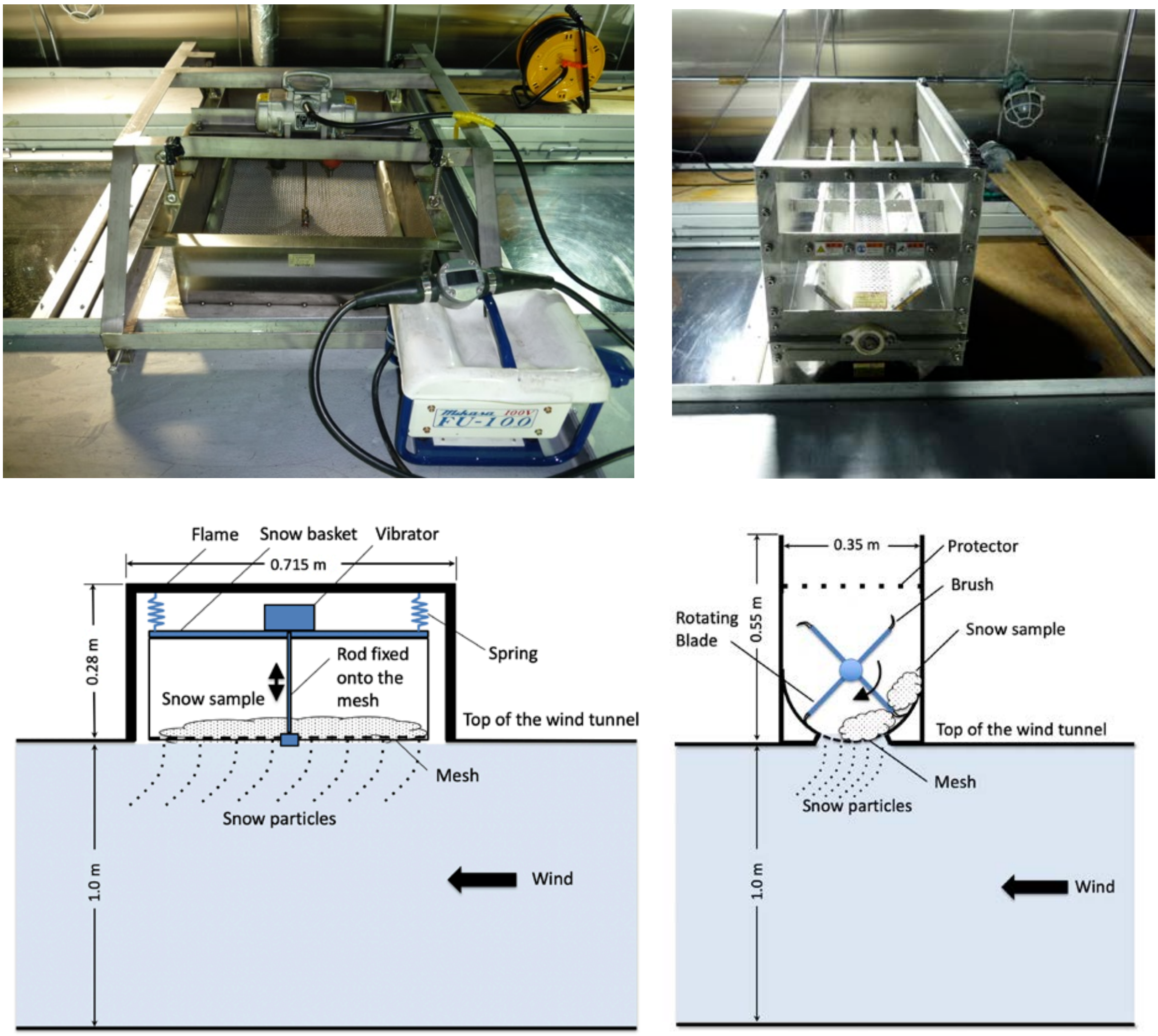

Fig. 8. Small snowfall machines used to sieve snow particles into the wind tunnel from the top window. Left: vibrational type, Right: rotating-brush type. Bottom figures show the snowfall machine schematics.

Full width

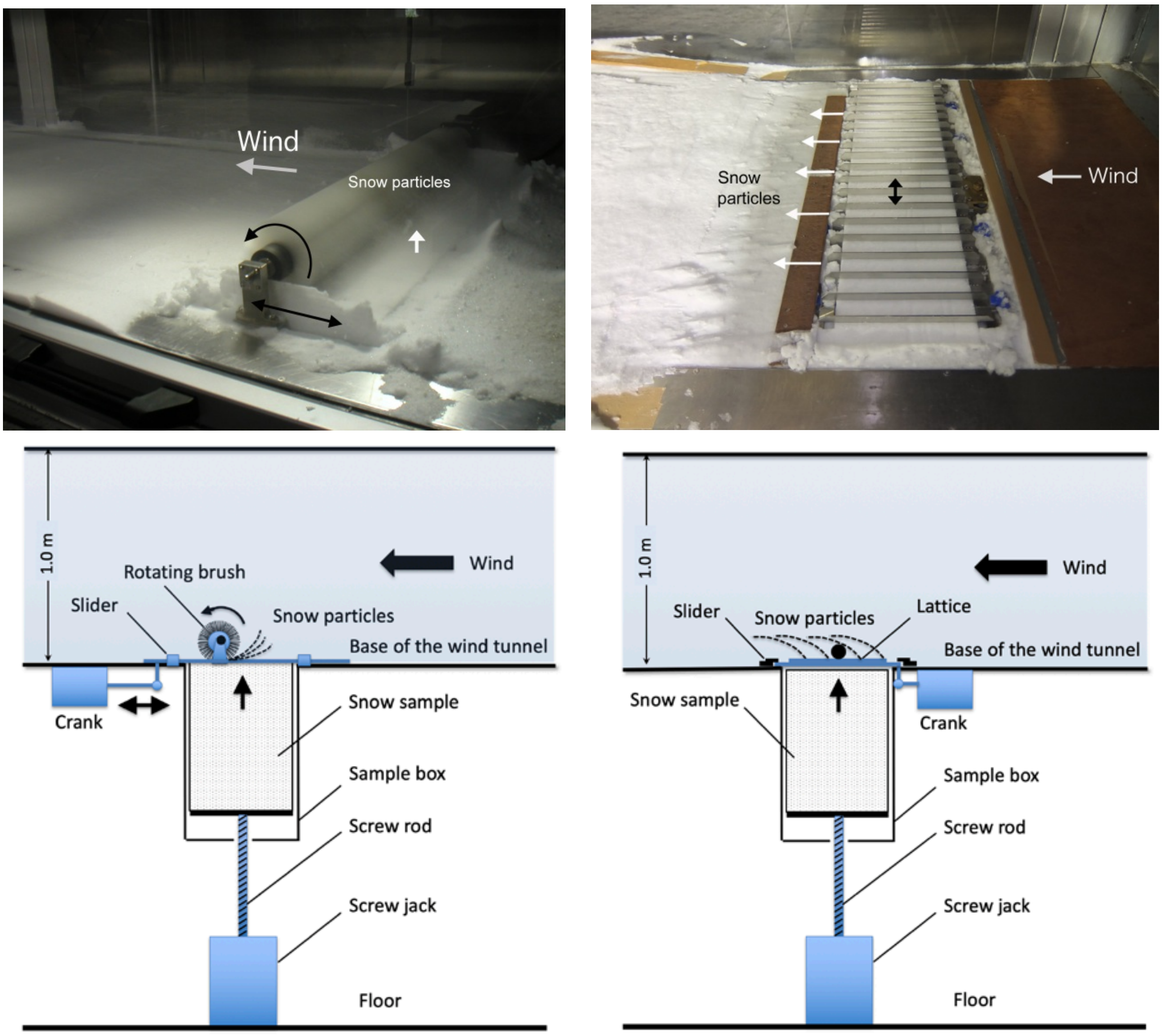

Fig. 9. Snow seeders in the wind tunnel. Left: rotating-brush type, Right: reciprocating type. Bottom figures show the snow seeder schematics. Dimensions of the sample box for both types are 0.2 m in length × 0.77 m in width × 0.3 m in depth.

Full width

Fig. 10. CES Control room. An operator (left) monitors the control panel and a technician (left back) supports data collection for the collaborators who typically provide their original instruments (right). The cold room can be seen through the window on the left.

Full width

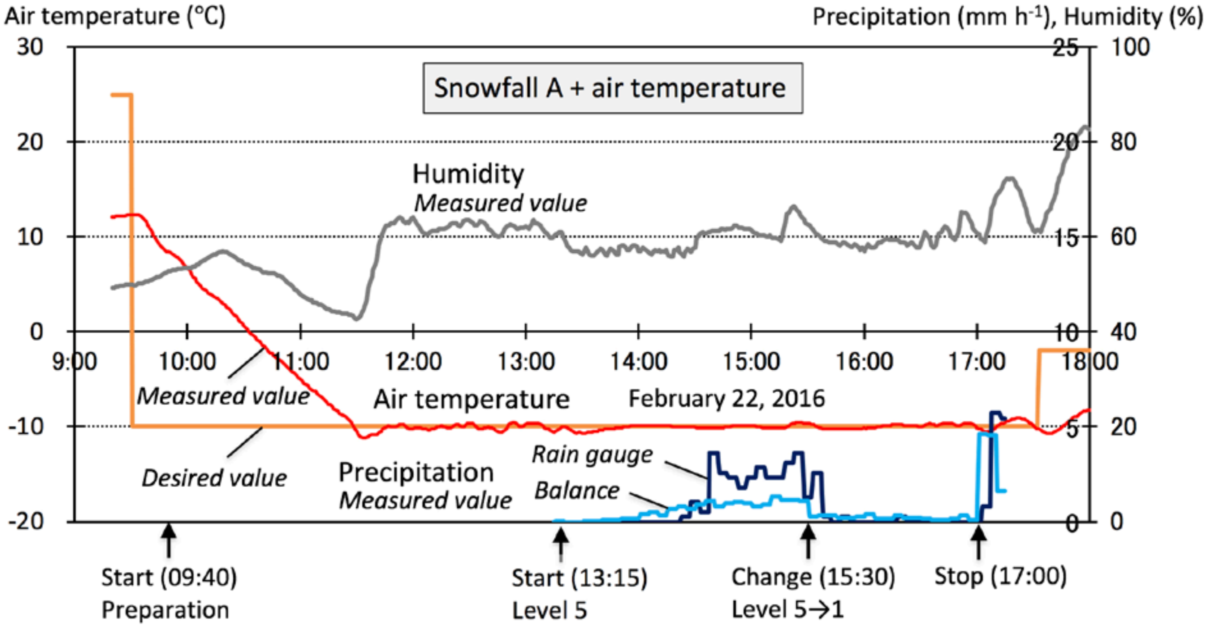

Fig. 11. Time series data for desired and measured precipitation of snowfall A and air temperature, in addition to measured humidity.

Full width

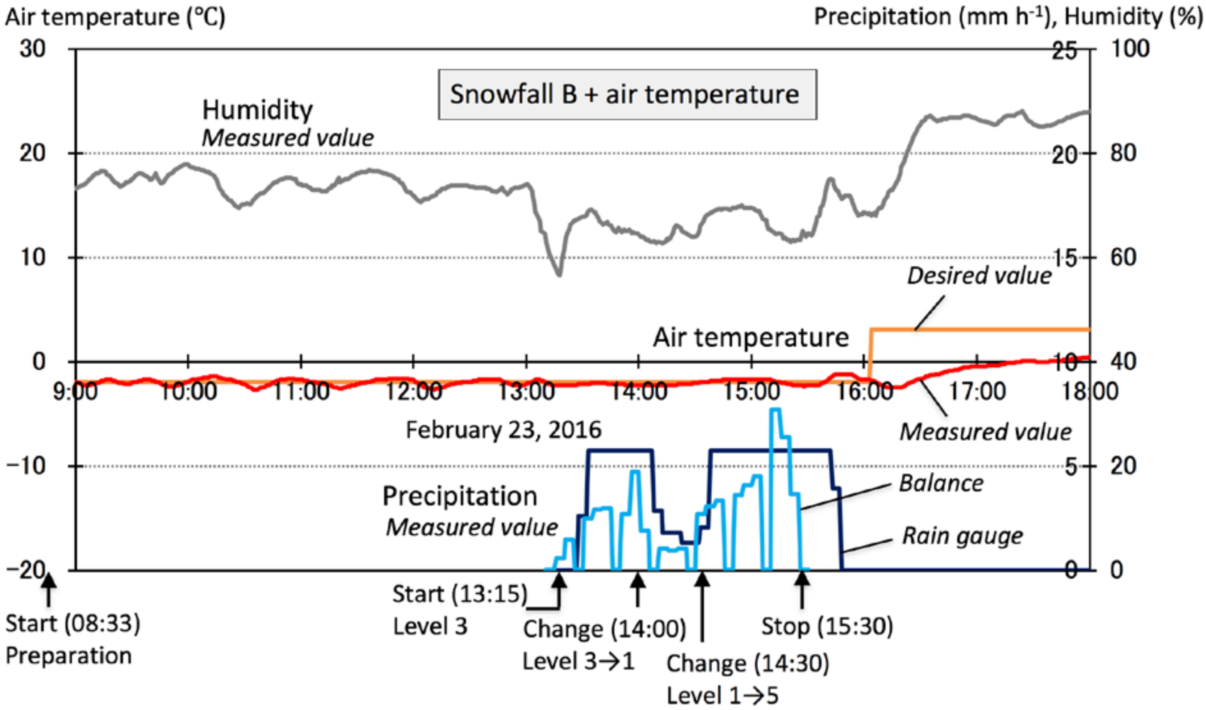

Fig. 12. Time series data for desired and measured precipitation of snowfall B and air temperature, in addition to measured humidity.

Full width

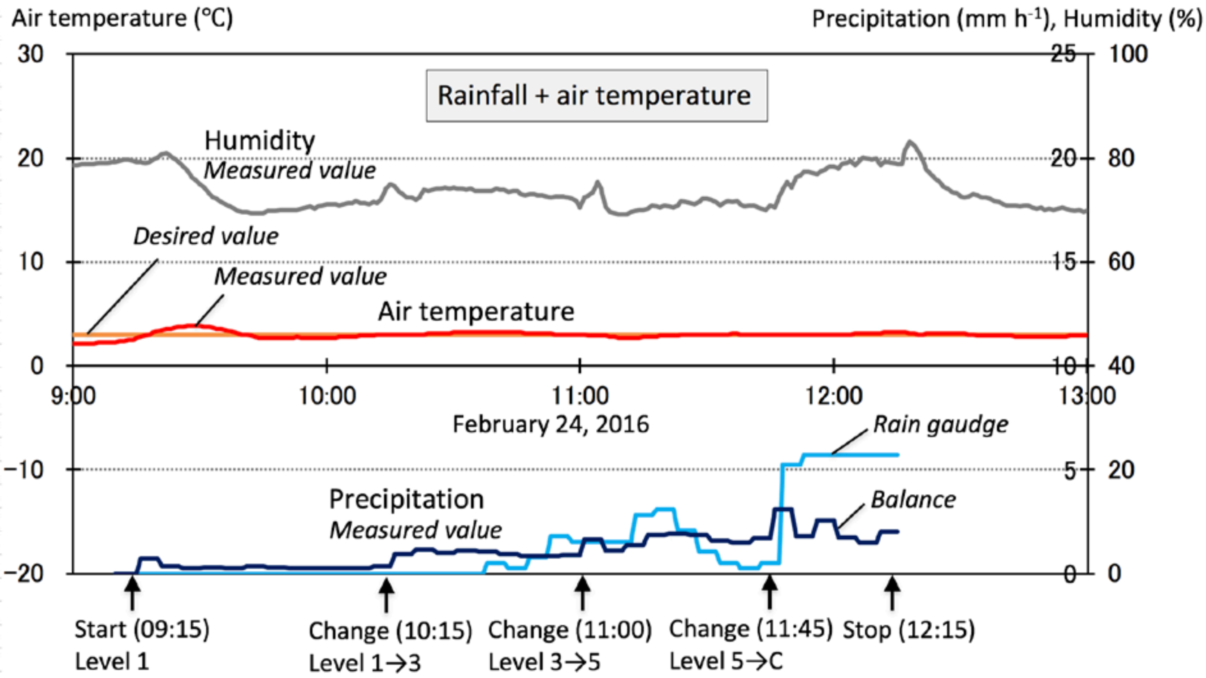

Fig. 13. Time series data for precipitation and air temperature. The numbers indicate the rainfall simulator level used to control the precipitation.

Full width

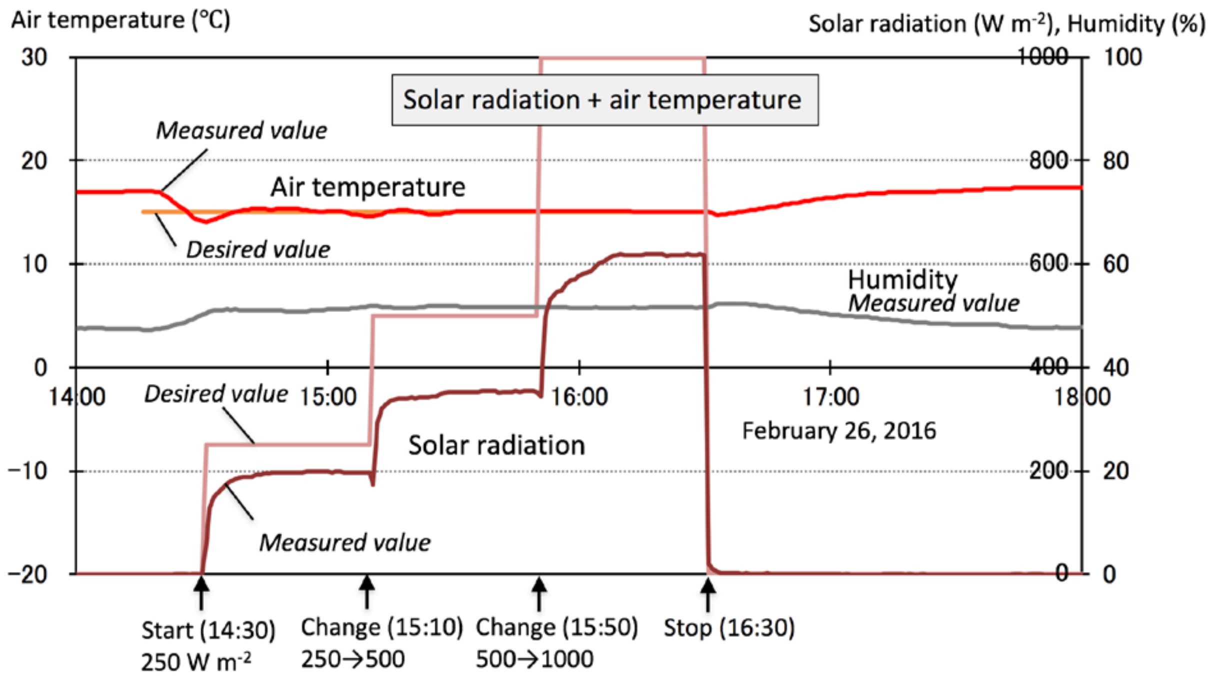

Fig. 14. Time series data for desired and measured solar radiation and air temperature controlled simultaneously.

Full width

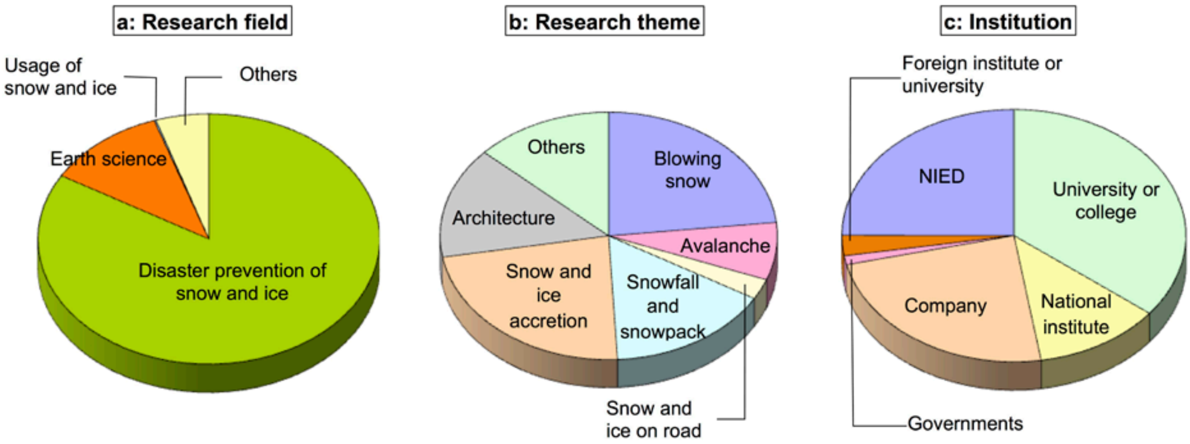

Fig. 15. Overview of the research field, theme, and institution.

Full width

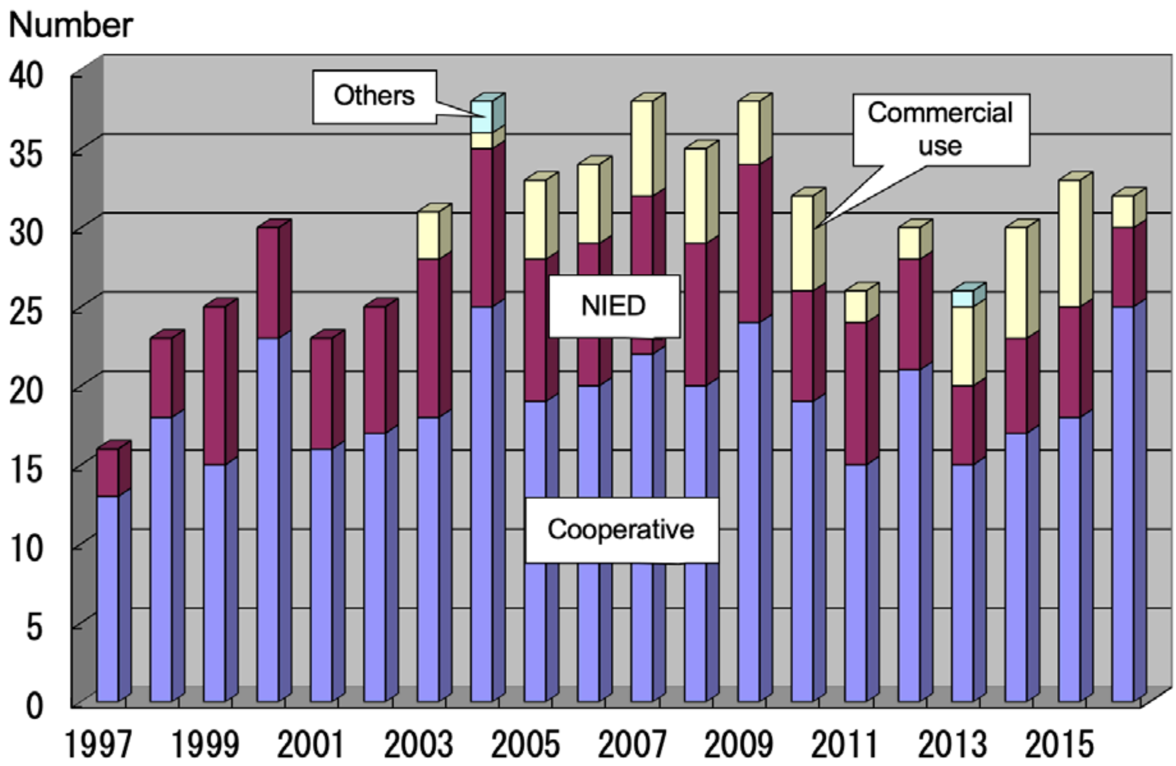

Fig. 16. Institutional categorization of projects conducted at the CES.

Full width